TASK QUARTERLY 8 No 3 (2004), 359–375

QUALITY ENHANCEMENT OF EDDY-CURRENT-BASED NON-DESTRUCTIVE EVALUATION DATA THROUGH INDEPENDENT COMPONENT ANALYSIS

EMILIANO FRULLONI AND SIMONE FIORI

Faculty of Engineering of the Perugia University,
Loc. Pentima bassa 21, I-05100 Terni, Italy
{frulloni, fiori}@unipg.it

(Received 23 January 2004)

Abstract: The aim of this paper is to examine the performance of an independent component analysis algorithm based on neural networks applied to the solution of an electrical engineering problem related to non-destructive evaluation of conductive objects. The proposed application is assessed through computer experiments carried out on real-world data, which prove the usefulness of this non-destructive evaluation technique.

Keywords: neural network applications, eddy-current testing, independent component analysis

1. Introduction

Blind signal processing by neural networks is an emerging research field which benefits from cross-fertilization among the scientific areas related to neurobiology, signal processing and adaptive circuits. In fact, intelligent signal/data processing tasks and adaptive circuits share fundamental goals with biological systems, such as universal data processing of multiple signals, unsupervised classification and supervised learning by examples. Thanks to these features, neural networks are attractive candidates for intelligent multiple signal processing, as evidenced by the recent research activity in this area.

In particular, blind source separation by the independent component analysis (ICA) has received much attention in the recent years owing to its potential applications to intelligent multiple signal processing, as in speech recognition systems, telecommunications, fault detection tasks, medical imaging, financial data analysis and other important research fields [1–4]. The aim of ICA is twofold: first, to recover unobservable independent source signals from their sensor observations by reducing high-order statistical correlations; second, to extract independent latent variables from structured signals by constructing few linear combinations of many measured signals that retain the largest quantity of information.

The pioneering work on ICA was carried out by Hérault and Jutten [5, 6], who introduced an adaptive algorithm in a feedback neuromimetic multiple filter; their approach was further developed by Cichocki and Umbehauen (see [7]). Comon [8] developed the concept of independent component analysis and proposed a class of cost functions termed discriminant contrasts. The contrast-based approach was further studied by Comon, Moreau and Macchi who introduced simplified contrasts for lepto-kurtic and plati-kurtic source signals (*i.e.* for signals with positive or negative kurtosis) [9, 10]. On the basis of simplified contrast (*i.e.* kurtosis optimization), Cardoso and Laheld [11] proposed an adaptive algorithm relying on the relative gradient, which has been proven to enjoy very desirable properties, such as equivariancy and fast convergence. In addition to these parallel algorithms, Delfosse and Loubaton [12] proposed an approach based on a deflation procedure, whose idea has been recently developed by Thawonmas, Cichocki and Amari, resulting in a cascade neural network [13]. Some algorithms are also available for hetero-kurtic ICA, *i.e.* in the case when source signals are mixed plati-kurtic and lepto-kutic signals (see [14–18] and references therein). Some non-iterative algorithms (*i.e.* block learning procedures) have also been proposed. (For an up-to-date review see *e.g.* the survey paper [19] and the recent proposal by Yeredor [20].)

In parallel to such ICA studies, unsupervised learning rules based on information theory were proposed by Linsker [21] and Plumbley [22]. Their aim was to maximize the mutual information between the inputs and the outputs of a neural network so that each neuron is able to encode features as statistically independent as possible from the features extracted by other neurons. Baram and Roth [23], and Bell and Sejnowski [24], derived stochastic gradient learning rules for this maximization and applied them to forecasting and time-series analysis, blind separation of sources and blind deconvolution, respectively. Girolami and Fyfe [25] employed neural exploratory projection pursuit algorithms to achieve separation. Generalized Hebbian learning algorithms for ICA have been developed by Karhunen *et al.* [26], Hyvärinen and Oja [27], and Fiori [28]. Non-conventional neural optimization techniques have recently been applied to blind separation; worth citing as representative examples are the mechanical-type learning algorithms of Fiori [29, 30], the purely geometrical approach to be applied in the presence of uni-modal/symmetrical source density distributions developed by Prieto *et al.* [31], the genetic algorithm by Yoshioka and Omatu [32] and the EM-type algorithm for independent component analysis developed by Welling and Weber [33].

Many experiments have been performed to illustrate the usefulness and effectiveness of separating algorithms, for instance in EEG data processing (showing that the algorithms can extract EEG activation and isolate artifacts), and in exploring independent features in natural images. Neural techniques have recently been applied to solve electromagnetic problems (see *e.g.* [34–36] and references therein), and it has been specifically proven in recent experimental research that the use of ICA enables one to acquire additional knowledge from electromagnetic measurements [37–40].

The aim of the present paper is to examine one of the sequential approaches to ICA, the TCA algorithm of Thawonmas, Cichocki and Amari [13], with application to the non-destructive evaluation of metallic slabs by eddy-current testing data analysis.

Eddy-current testing (ECT) [41, 42] is a non-destructive evaluation (NDE) technique especially well suited for inspection of metallic objects with a probe system. The probe is connected to a digital nano-voltmeter, capable of measuring complex-valued voltage. Voltage change is used for defect detection and identification, with particular interest in defect shape. When a defect is present in a slab, it is important to detect, localize and measure the crack. However, eddy-current measurement is corrupted by the skin effect, the lift-off disturbance and measurement noise. Prior to the development of a flaw detection/recognition system, the measure has to be restored by featuring the disturbance and the defect signal. In order to extract information from the measured data, a proper signal processing algorithm based on ICA is proposed and tested on real-world data made available by the Hungarian Academy of Sciences.

2. Independent component analysis

2.1. Signal model and independence

Let us assume that n linear mixtures $x_1(t),\ldots,x_n(t)$ of m $(m \leq n)$ independent components $s_j(t)$ are observed. Let us further assume $s_j(t)$ to be unknown random signals:

$$x_j(t) = a_{j1}s_1(t) + a_{j2}s_2(t) + \ldots + a_{jm}s_m(t), \quad j = 1,\ldots,n \tag{1}$$

or, using a matrix notation:

$$\mathbf{x}(t) = \mathbf{A}\mathbf{s}(t). \tag{2}$$

Note that, in general, the t variable denotes a data ordering index, such as a discrete-time or a spatial index.

If the elements of matrix $\mathbf{A}$ are known, in order to extract s_j it would suffice to solve the linear equation system described by Equation (2). If matrix $\mathbf{A}$ is also unknown, s_j's appear as latent variables, which means that they are not directly observed, and a different way has to be pursued to solve the problem. In particular, independent component analysis (ICA) allows one to calculate $s_j(t)$ and the mixing matrix $\mathbf{A}$ from the observed signals $x_1(t),\ldots,x_n(t)$ only under fair conditions.

The main hypotheses about the signal model are: (1) each $s_j(t)$ is an independent, identically distributed (IID), stationary, random process; (2) $s_j(t)$'s are statistically independent at any time; (3) at most one among the source signals has a Gaussian distribution; (4) $\mathbf{A}$ is a constant, real-valued, full-rank matrix. The basic ICA theory shows that, under the above conditions, the sources may be recovered up to arbitrary scaling and permutation [8].

An interesting example to explain the blind separation problem is the "cocktail party" scenario [24]. Let us imagine m people standing in a room and talking. If the room is equipped with n microphones, each sensor receives a different superposition of the speech signal uttered by each person in the room, so that the set of received signals may be described by model (2), where matrix $\mathbf{A}$ describes the geometry of "emitters" and the sensor and pressure wave propagation phenomena. The aim is to recover, from sensor observation only, single independent signals uttered by the people. This is a source separation problem in that we know that there exist some sources which physically emit some signals that impinge on an array of sensors.

The idea behind latent variable extraction is quite different: given a multivariate signal having complex structure, the aim is to construct a set of signals (latent

variables) endowed with special features whose linear superposition described by (2) gives the observed signals. Latent variables may have no recognizable physical meaning and we require they have the special feature to be as statistically independent as possible. An example to clarify the concept of latent variables extraction is the analysis of vibrating machines [43]. Let us suppose that a rotating pump under fault test is equipped with a number of accelerometers that measure its vibration amplitudes versus time. We know that the recorded accelerometer signals are originated by a large number of small vibrating parts. Seeking for a compact representation of the measured data by the ICA technique, the obtained basis of independent signals are (complex) vibration-signals pertaining to a small number of *virtual* oscillators whose linear superpositions generate the observed data. The classification of vibration modes of these virtual oscillators leads to an effective fault-detection technique.

Although in the above examples we have started from two different perspectives, the assumed signal model is the same and, thus, the solution is the same. Independent component analysis provides an interesting and effective solution to such problems.

ICA is based on the concept of independence. Two random variables, y_1 and y_2, are termed statistically independent if the knowledge of the value of one of them does not help us in any way to know the value of the other. From this property we can also derive the following relation:

$$E\{h_1(y_1)h_2(y_2)\} = E\{h_1(y_1)\}E\{h_2(y_2)\}, \tag{3}$$

where h_1 and h_2 are generic functions and $E\{\cdot\}$ denotes statistical expectation. This relation is stronger than the un-correlation between variables expressed as:

$$E\{y_1y_2\} - E\{y_1\}E\{y_2\} = 0. \tag{4}$$

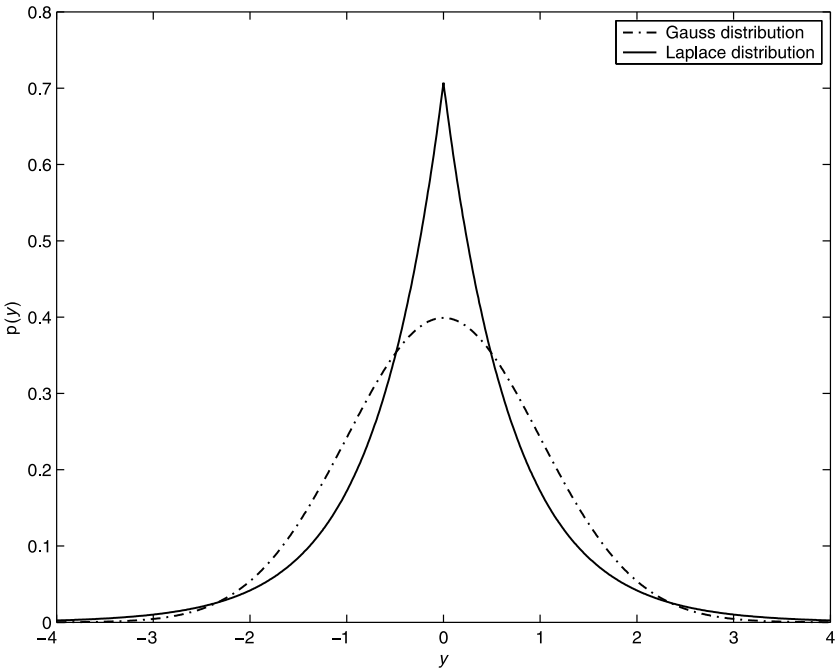

Figure 1. Comparison between the density function of Gaussian and Laplacean distributions

To perform ICA statistical independence of signals is necessary (for them to be extracted) and, from the distribution point of view, their non-Gaussianity. To illustrate the non-Gaussianity aspect, we refer the reader to the example used by Hyvärinen and Oja in [44]; in Figure 1 the density function of a Gaussian distribution:

$$p(y) = \frac{1}{\sqrt{2\pi}} \exp\left(-\frac{y^2}{2}\right), \tag{5}$$

and that of a Laplacean (*i.e.* super-Gaussian) distribution:

$$p(y) = \frac{1}{\sqrt{2}} \exp\left(-\sqrt{2}|y|\right), \tag{6}$$

are compared, both normalized to unit variance.

A classical measure of non-Gaussianity is the kurtosis or fourth-order cumulant, defined for a random variable y as:

$$kurtosis(y) = E\{y^4\} - 3(E\{y^2\})^2. \tag{7}$$

From this definition we derive the following properties:

$$\begin{aligned} kurtosis(y_1 + y_2) &= kurtosis(y_1) + kurtosis(y_2), \\ kurtosis(ay) &= a^4 kurtosis(y), \end{aligned} \tag{8}$$

for any pair of independent signals, $y_1(t) \in \mathbb{R}$, $y_2(t) \in \mathbb{R}$, and for any constant $a \in \mathbb{R}$.

The value of the *kurtosis* gives rise to a signal classification. It is:

- **positive** if the distribution is super-Gaussian,
- **negative** if the distribution is sub-Gaussian,
- **zero** for a Gaussian distribution.

Kurtosis' response to signal Gaussianity does not change if we consider its normalized form:

$$\overline{kurtosis}(y) = \frac{E\{y^4\}}{(E\{y^2\})^2} - 3. \tag{9}$$

In this case the properties described in Equation (8) are recast in the following form:

$$\begin{aligned} \overline{kurtosis}(y_1 + y_2) &= \overline{kurtosis}(y_1) + \overline{kurtosis}(y_2), \\ \overline{kurtosis}(ay) &= \overline{kurtosis}(y). \end{aligned} \tag{10}$$

2.2. Independent component analysis with a cascade neural network

Many algorithms based on neural networks have been developed to perform independent component analysis. Thawonmas, Cichocki and Amari have proposed in [13] the use of a cascade neural network giving rise to a separation procedure hereafter referred to as a TCA algorithm. An exemplary schema of such a network with five different input signals is show in Figure 2. We can assume without a loss of generality to have a zero-mean random vector $\mathbf{x} = [x_{11}(t), \ldots, x_{15}(t)]^T$ of unit covariance at the input.

The algorithm will work so that the extraction unit shown in Figure 2 will evolve, in the value of $(w_1, \ldots, w_5)$, until one of s_k's will be extracted. This means having $y_1(t) = \pm c s_k(t)$, with $c \in \mathbb{R}^+$. At this point a deflation process will take place

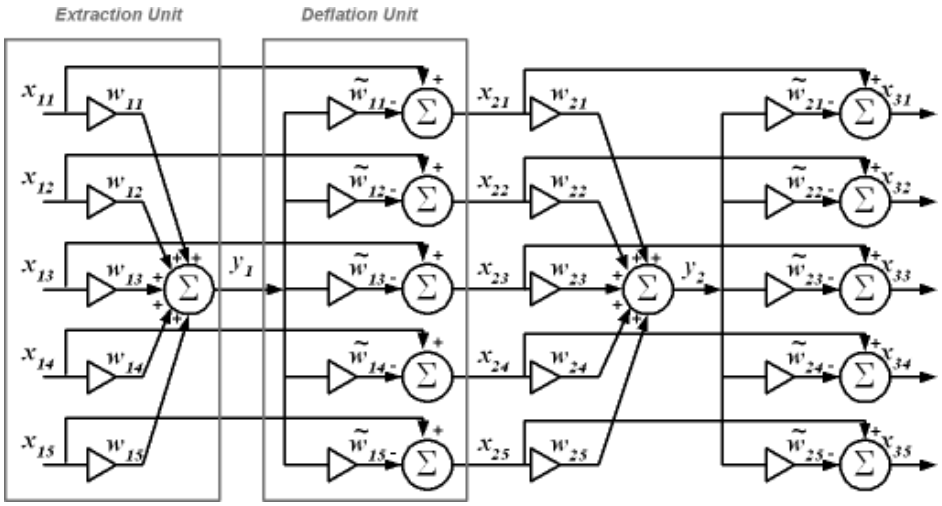

Figure 2. Cascade neural network described in [13] (the case with five input signals)

in order to obtain a new vector, $[x_{21}(t),\ldots,x_{25}(t)]^T$, of signals that are linear mixtures of components not yet extracted. New extraction and deflation units will follow until the last independent component has been extracted.

It is important to underline that, in general, the observed signals do not meet all the above conditions. However, it is always possible to remove the first- and second-order statistics from the observations in order to make them zero-mean and uncorrelated, as explained in the following section.

The TCA algorithm is based on minimization with respect to weight, $\mathbf{w}_k$, of the normalized cost function:

$$\mathcal{J}(\mathbf{w}_k) = \frac{1}{4}\beta\overline{kurtosis}(y_k), \tag{11}$$

where:

$$\beta = \begin{cases} +1 & \text{for extraction of a source signal with negative } \textit{kurtosis} \\ -1 & \text{for extraction of a source signal with positive } \textit{kurtosis} \end{cases}$$

This determines the law for the evolution of weight, $\mathbf{w}_k$, during the extraction process to be [13] as follows:

$$\frac{d\mathbf{w}_k}{dt} = -\mu_k(t)\left[\frac{E\{y_k(t)^4\}}{E\{y_k(t)^2\}^3}\right]\left[y_k(t) - \frac{E\{y_k(t)^2\}}{E\{y_k(t)^4\}}y_k^3(t)\right]\mathbf{x}_k(t). \tag{12}$$

It is important to note that the sign of the kurtoses of the independent signals to be extracted is unknown, therefore the algorithm estimates it on the basis of the current source estimation provided by the neuron. The above learning rule incorporates such a sign estimation technique.

In the above learning equation, $\mu_k(t)$ is a time-dependent learning rate of the following expression:

$$\mu_k(t) = \mu_1 \exp\left[\log\left(\frac{\mu_2}{\mu_1}\right)\frac{t}{T_{\max}}\right] \tag{13}$$

of the shape shown in Figure 3.

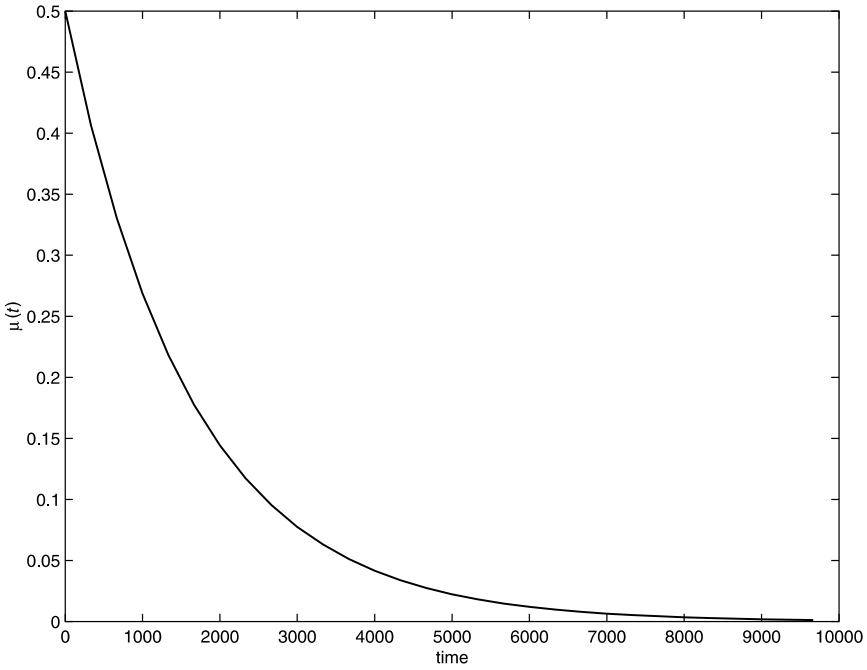

Figure 3. Learning rate $\mu_k(t)$

As can be seen from Equation (13), the learning rate is completely defined once the value of μ_1 and μ_2 have been chosen. The influence of these two parameters on the behavior of $\mu_k(t)$ is presented in Figures 4 and 5. The $T_{\max}$ quantity denotes the maximum temporal abscissa of the signal.

The learning Equation (12) enables the k^{th} neuron to extract an independent component from the residual mixture $\mathbf{x}_k(t)$, which is obtained by deflating the residual mixture $\mathbf{x}_{k-1}(t)$ from the $(k-1)^{\text{th}}$ independent component, where, $\mathbf{x}_1(t)$ by convention coincides with the original observations. We can formally define the $\mathbf{x}_k(t)$ sequence as:

$$\begin{aligned} \mathbf{x}_1(t) &= \mathbf{x}(t), \\ \mathbf{x}_{k+1}(t) &= \mathbf{x}_k(t) - \tilde{\mathbf{w}}_k y_k(t), \quad k \geq 1. \end{aligned} \tag{14}$$

The $\tilde{\mathbf{w}}_k(t)$ vector is termed a "signature" of the extracted source and should coincide with one of the columns of the mixing matrix $\mathbf{A}$, up to a scale factor and a possible sign switch. The signature vector may be computed on the basis of simple least-mean-square produces described in [13].

2.3. TCA algorithm tested on images

In a way similar to that presented in [13], the behavior of the cascade neural network proposed by Thawonmas, Cichocki and Amari has been investigated with respect to image extraction from mixed combinations. The TCA algorithm's performance has been assessed for the case of a number of mixtures equal to the number of independent components. These experiments were performed in order to examine the TCA algorithm's performance on a synthetic problem and to validate the learning-rate decaying-scheme in order to find suitable learning values μ_1 and μ_2 for the subsequent ECT/NDE data processing.

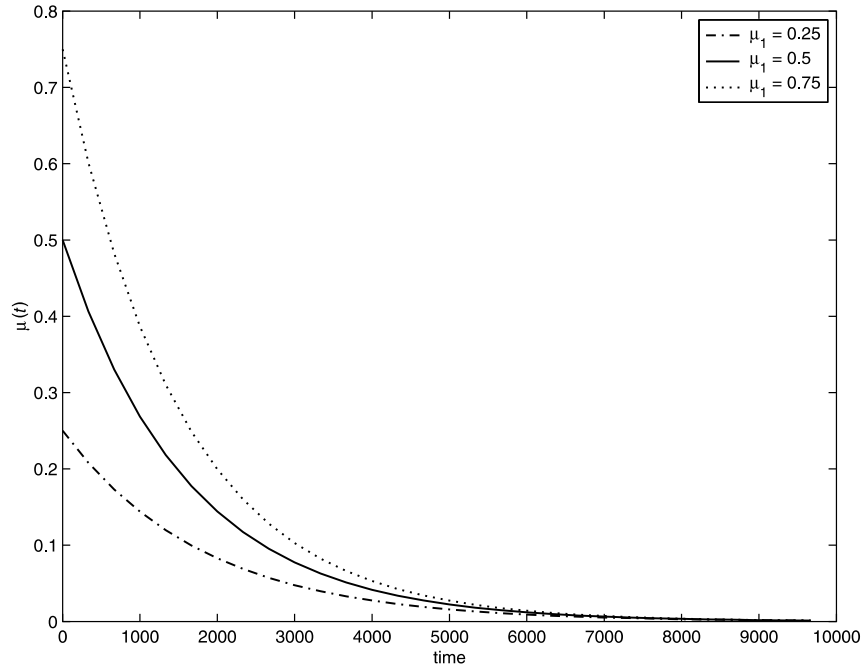

Figure 4. Impact of μ_1 variation on $\mu(t)$ ($\mu_2 = 0.001$)

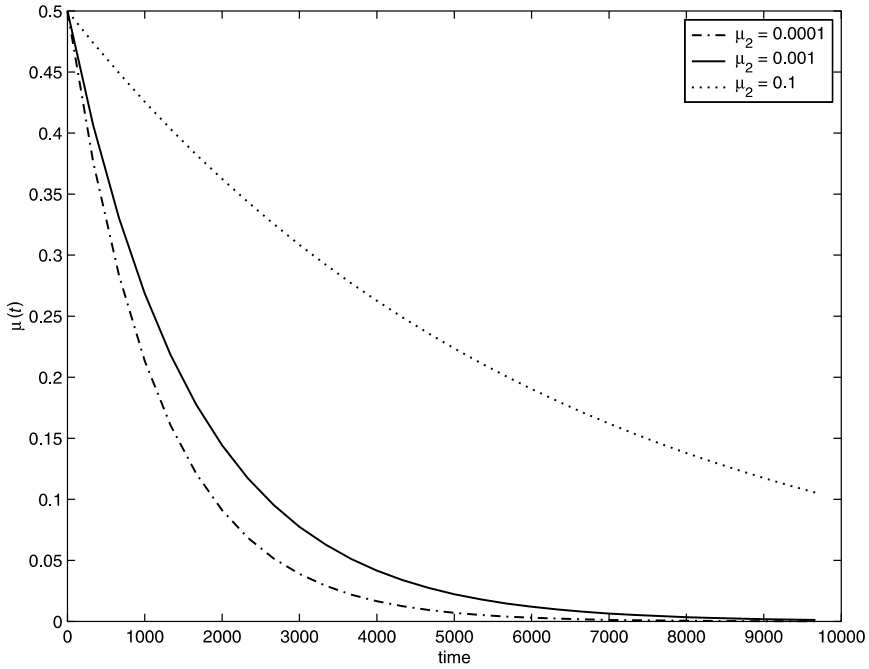

Figure 5. Impact of μ_2 variation on $\mu(t)$ ($\mu_1 = 0.5$)

Images presented in Figure 6 have been used for the test. The five original images are 100×100 gray-level pictures with both negative and positives kurtoses of the following normalized values: -1.67, 1.98, -0.84, -0.78 and 0.4. Five linear

mixtures were generated from the original images (see Figure 6) by multiplying the source signal vector $\mathbf{s}$ by the randomly generated mixing matrix $\mathbf{A}$:

$$\mathbf{A} = \begin{pmatrix} 0.9003 & 0.5242 & 0.2309 & -0.1886 & -0.8842 \\ -0.5377 & -0.0871 & 0.5839 & 0.8709 & -0.2943 \\ 0.2137 & -0.9630 & 0.8436 & 0.8338 & 0.6263 \\ -0.0280 & 0.6248 & 0.4764 & -0.1795 & -0.9803 \\ 0.7826 & -0.1106 & -0.6475 & 0.7873 & -0.7222 \end{pmatrix}$$

The obtained mixed signal vector, $\mathbf{x}(t) = [x_1(t), \ldots, x_5(t)]^T$, was then pre-processed before inputting into the neural network. It was first centered by subtracting its mean value:

$$\mathbf{x}_c = \mathbf{x} - E\{\mathbf{x}\}. \tag{15}$$

The resulting vector-stream is then whitened, *i.e.* a new vector, $\mathbf{x}_c^w$, is obtained from $\mathbf{x}_c$ (with a linear transformation) whose components are uncorrelated and have unit variance. To perform whitening, we used the method based on eigenvalue decomposition (EVD). Starting from an eigenvector matrix $\mathbf{E}$ and a diagonal eigenvalue matrix $\mathbf{D}$ of $E\{\mathbf{x}_c\mathbf{x}_c^T\}$, asymmetric whitening is performed by:

$$\mathbf{x}_c^w = \mathbf{D}^{-1/2}\mathbf{E}^T\mathbf{x}_c, \tag{16}$$

where $\mathbf{D}^{-1/2} = \operatorname{diag}\left(d_1^{-1/2}, \ldots, d_n^{-1/2}\right)$.

The pre-whitening has the effect of making the data better conditioned for the processing phase that follows and accelerating the network learning phase [1]. Once centered and whitened, the signal is processed using the TCA algorithm. Figure 6 shows the original, mixed and extracted images. These results pertain to the values of:

$$\begin{cases} \mu_1 = 0.5, \\ \mu_2 = 0.001. \end{cases} \tag{17}$$

The influence of the values of μ_1 and μ_2 on the performance of the algorithm was tested within the range $[0.0001, 0.1]$ for μ_2 and $[0.25, 0.75]$ for μ_1 (see Figures 4 and 5). We found a stronger dependency of the results on the value of μ_2, with respect to the influence of parameter μ_1, that had no influence. The best results were found, on average, using the pair of values of Equation (17) (see Figure 7).

3. Application to non-destructive evaluation problem

The physical phenomenon of eddy-currents is used as the basis for a non-destructive evaluation (NDE) technique usually referred to as eddy-current testing (ECT) to inspect metal parts. The technique is based on measurement of the impedance of a coil situated close to the surface to be inspected. The coil is driven by a sinusoidal current of a few mA of amplitude, with a frequency of less than 100 kHz, and is moved along the part's surface. The impedance of the circuit depends on the interaction of the metallic part under inspection with the magnetic field generated by the inductor. The presence of a crack on the surface or inside the metal causes a variation of the probe's resistance and inductance.

For instance, for a small spherical (point) void defect, the relationship between the differential impedance measured at a point of the specimen's accessible surface and the location of the imperfection has been derived by Prince and Hildebrand [45]

Figure 6. Computer simulation results for a mixture of image signals: original, mixed and extracted images (set of test images used in [16])

under the assumption that the probe is axially symmetric, driven with a sinusoidal current of constant amplitude, I, and angular frequency, ω, and that the metal is non-magnetic. Basic electromagnetic considerations suggest that the probe response, described by the value of its impedance change ΔZ, reads:

$$\Delta Z = -\frac{1}{I^2}\int_{\mathcal{V}_\Gamma} \mathbf{E}_i^T \mathbf{J}_d dv, \tag{18}$$

where $\mathbf{E}_i$ is the incident electric field, $\mathcal{V}_d$ is the defect volume, and $\mathbf{J}_d$ is the volume-current in the defect, which may be written as $\mathbf{J}_d = -\sigma \mathbf{E}_d$, with $\mathbf{E}_d$ being the electric field in the defect volume and σ representing the metal specimen's conductivity. When the defect has a diameter much smaller than the wavelength λ, it can be analytically shown that $\mathbf{E}_d = 1.5\mathbf{E}_i$, where $\mathbf{E}_i$ remains constant within the defect's volume. The complex incident electric field may be computed quite easily in this ideal setting and, after the electrical and magnetic properties of the metal are specified, the Prince-Hildebrand model allows one to compute the differential impedance, $\Delta Z(x_p, y_p, x_d, y_d, z_d)$, when the probe is located at (x_p, y_p)

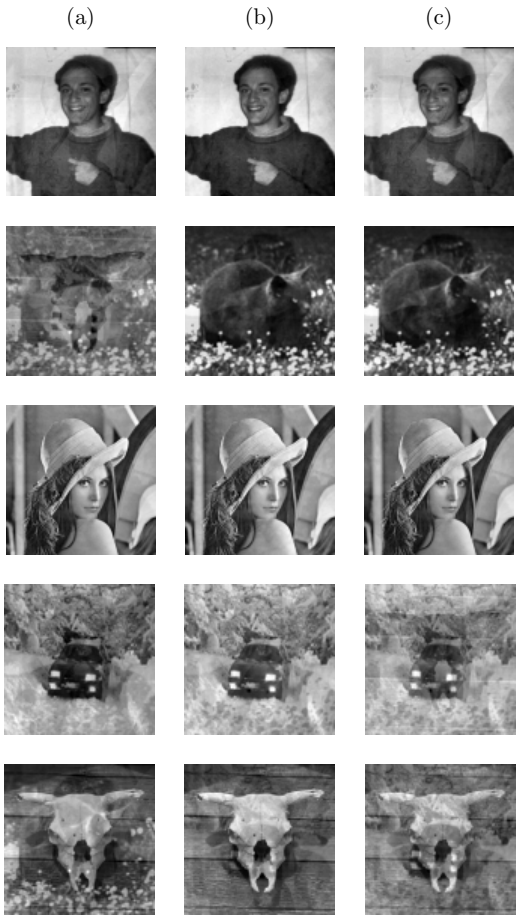

Figure 7. Sets of images extracted using different values of μ_2 in the neural network's settings: (a) $\mu_2 = 0.0001$, (b) $\mu_2 = 0.001$, (c) $\mu_2 = 0.1$; $\mu_1 = 0.5$ set for all runs

on the accessible specimen's surface and the defect is in (x_d, y_d, z_d). An exemplary theoretical differential impedance profile is depicted in Figure 8.

Eddy-current measurements are corrupted by the skin effect, lift-off noise due to the mechanical system and uncorrelated noise, and practical set-up measurement systems often display rather low signal-to-noise ratio values. Independent component analysis can be used in order to extract the component due to the defect from the measured signal, thus improving the signal-to-noise ratio for subsequent processing.

In order to better understand eddy-current test results, the MANODET (MAgnetic NOn DEstructive Testing) project was started in 1998. The project has been based on international collaboration of Universities. The Technical University of Budapest has built the probe and carried out the measurements. The obtained data have been distributed to other Universities to be analyzed. The tested specimen consists of a square INCONEL plate ($80 \times 80 \times 1.25$mm) with a rectangular thin crac in the center (0.2mm thick, 9mm long, 0.25mm deep); a schema of the specimen is shown in Figure 9.

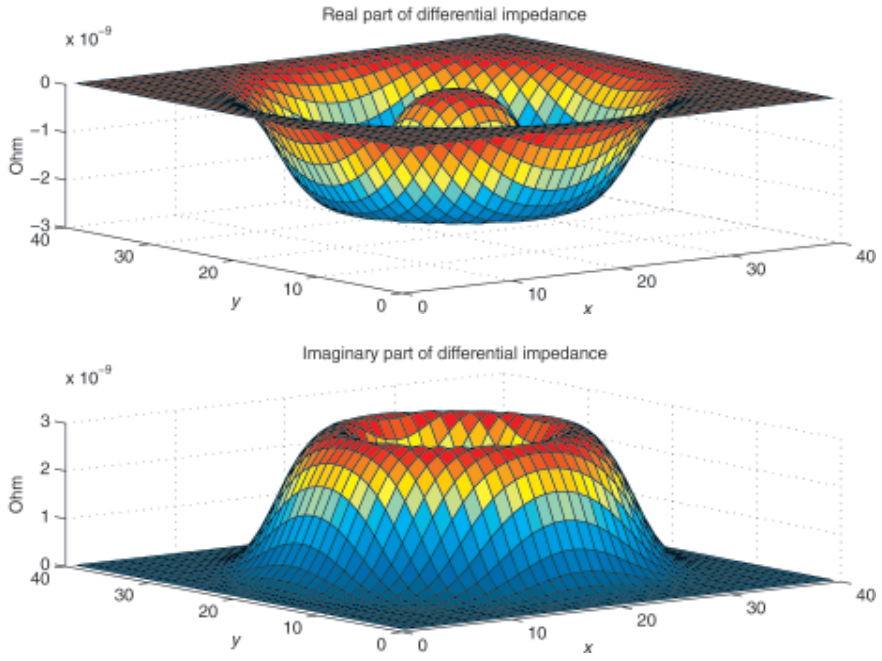

Figure 8. Exemplary differential impedance profile. In the example, the defect is located in (20,20) mm at a depth of 2 mm

From the inspection point of view, the crack can be a surface, outer defect (OD), or a hidden, inner defect (ID). The inspected area consists of a square region of 40×40 mm around the crack.

Figures 10 and 11 present measurements results in the case of an inner and an outer defect, respectively. The values refer to the magnitude and phase of the ECT-NDE complex signal. In order to carry out the signal restoration task, we have used a source-separation model. Our basic assumption has been that the measured signal is a linear superposition of two (complex-valued) signals: one due to the defect and the other coming from the lift-off noise and other disturbances. To perform an ICA, we have assumed that the real and imaginary parts of the involved signals interact in an additive way, and that the defect-signal and the disturbances are mutually statistically independent. The input signal to the neural network is then obtained as:

$$\mathbf{x} = \begin{bmatrix} |V_{ID}|\cos[\arg(V)_{ID}] \\ |V_{OD}|\cos[\arg(V)_{OD}] \\ |V_{ID}|\sin[\arg(V)_{ID}] \\ |V_{OD}|\sin[\arg(V)_{OD}] \end{bmatrix}. \tag{19}$$

The algorithm was also run with the validated parameter values of $\mu_1 = 0.5$, $\mu_2 = 0.001$. The four components extracted by the TCA neural network are show in Figure 12. One can see from Figure 12 that the algorithm has been able to separate the component due to the defect from the lift-off signal. Furthermore, the obtained component for the defect shows a good signal-to-background-noise ratio (see Figures 13 and 14).

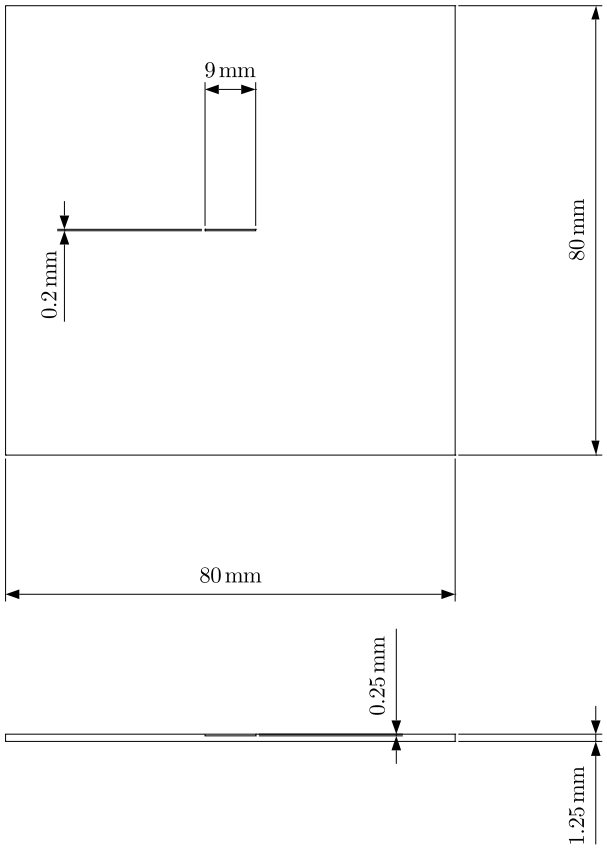

Figure 9. Schematic of the tested specimen for the ECT problem under investigation

The achieved separation between the defect signal and the background/lift-off disturbances would allow subsequent data processing enabling the ECT system to locate, describe and classify the crack in the material.

4. Conclusion

The behavior of the TCA algorithm of Thawonmas, Cichocki and Amari [13], based on a cascade neural network, has been considered within the independent component analysis scenario. Using images in a way similar to that of [13], the performance of the algorithm has been investigated in the case of the number of available signals equal to the number of independent components to be extracted. The influence of the learning parameters on the algorithm's performance has also been studied in order to find the best setting for the neural network. Furthermore, the TCA algorithm has been applied to the ECT-NDE data belonging to the MANODET project in order to separate the signal due to the presence of a defect from spurious components. The obtained results are satisfactory, as the algorithm has been able to point out the latent component relative to the presence of the defect with respect to the signal due to lift-off. The component extracted for the defect additionally shows a good ratio between the signal and the background-noise.

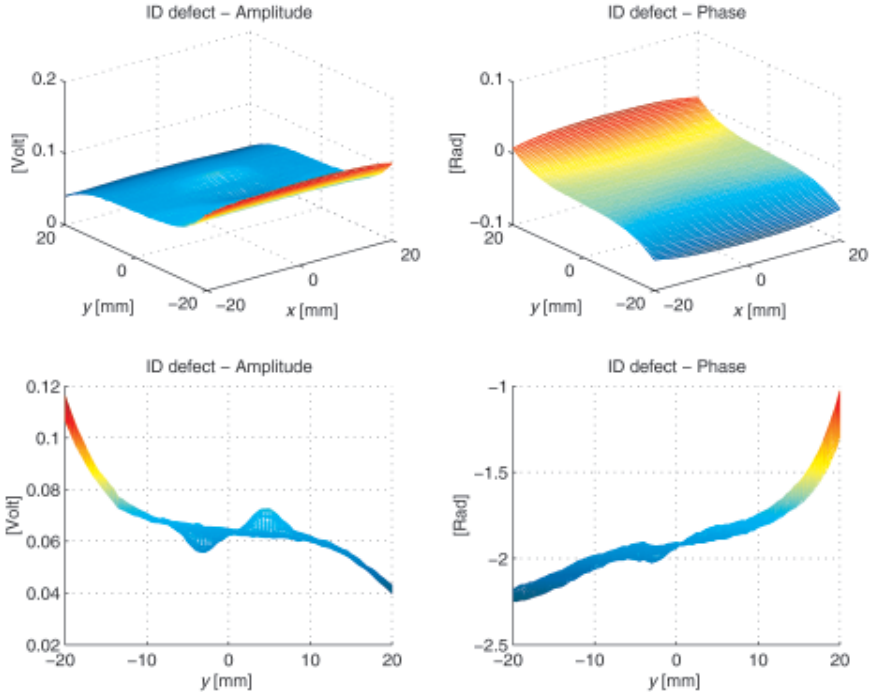

Figure 10. Magnitude and phase of a ECT-NDE signal for an inner defect (ID); two different views

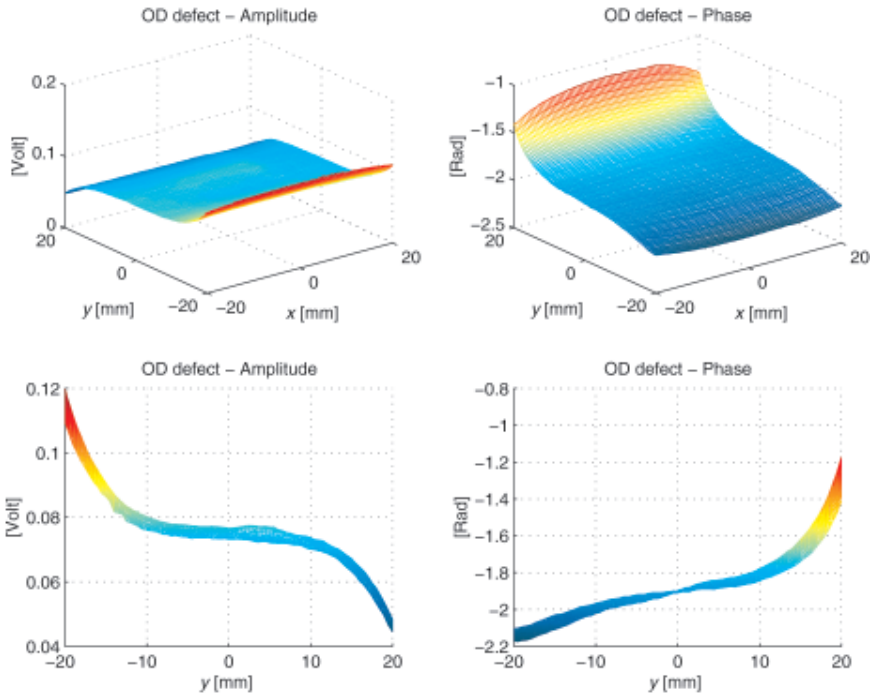

Figure 11. Magnitude and phase of a ECT-NDE signal for an outer defect (OD); two different views

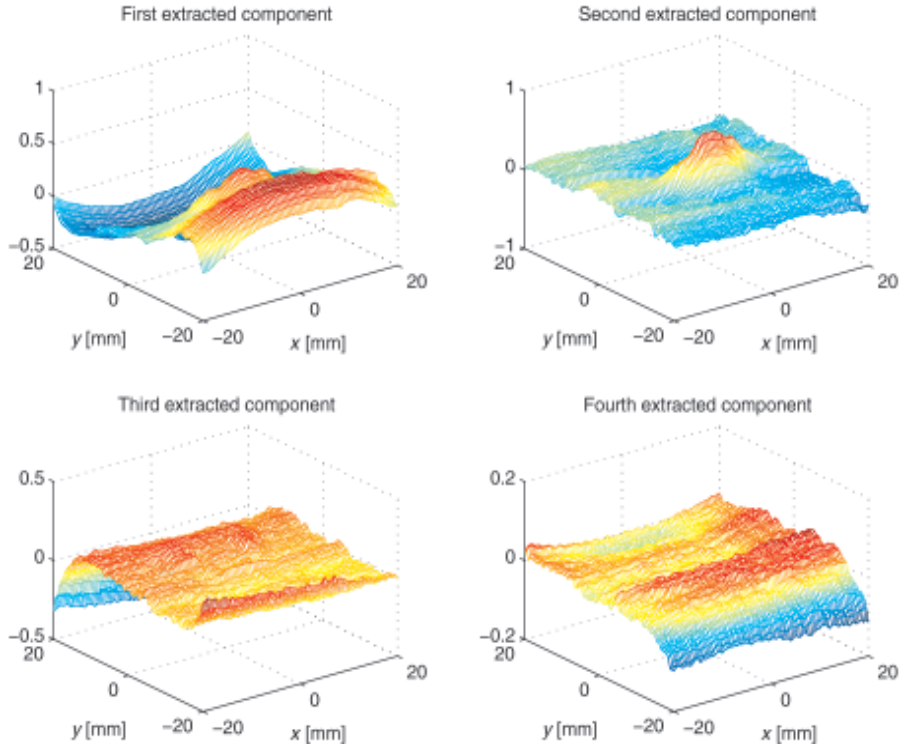

Figure 12. Estimated latent variables in the NDE problem as extracted by the TCA algorithm

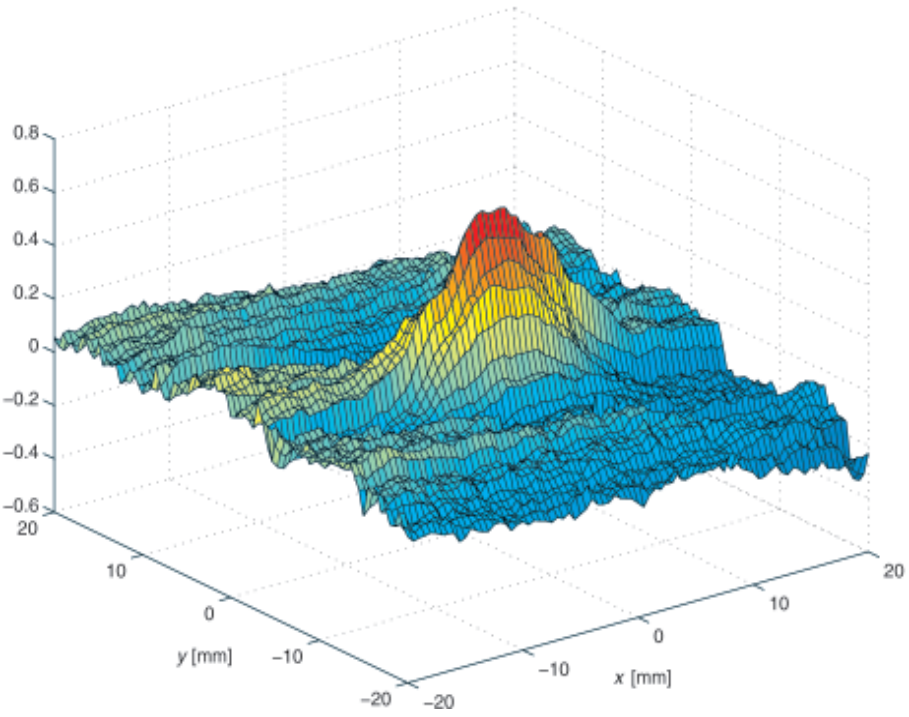

Figure 13. Estimated latent variable in the NDE problem corresponding to the defect signal

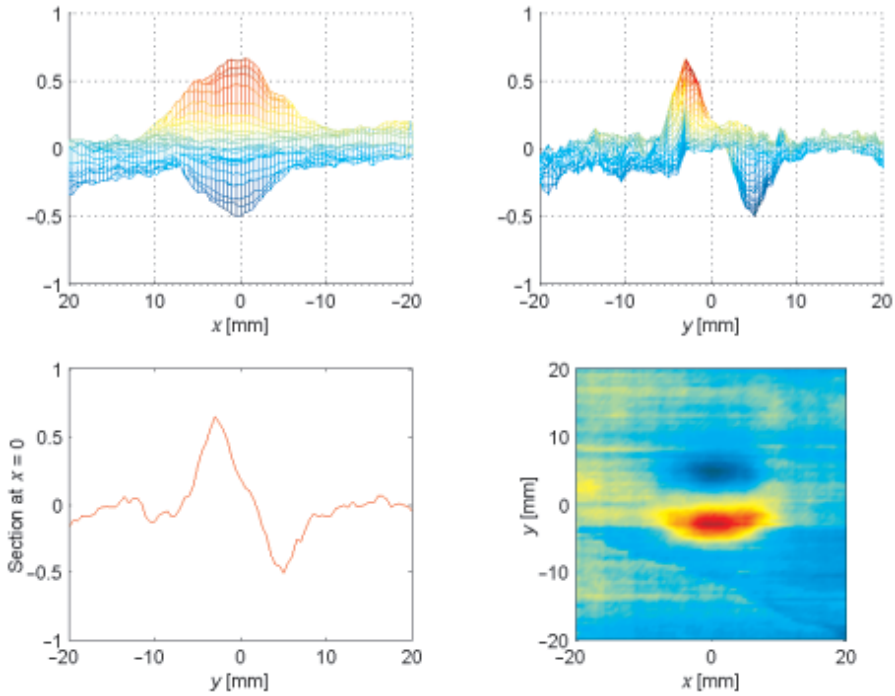

Figure 14. Different views of the component due to the defect

References

[1] Giannakopoulos X, Karhunen J and Oja E 1999 *Int. J. Neural Systems* **9** (2) 99
[2] Karhunen J, Hyvärinen A, Vigário R, Hurri J and Oja E 1997 *Proc. Int. Conf. on Acoustics, Speech and Signal Processing, ICASSP*, Münich, Germany, pp. 131–134
[3] Lee T-W 1998 *Independent Component Analysis – Theory and Practice*, Kluwer Academic Publisher
[4] Liu R W 1996 *Proc. Int. Symposium on Circuits and Systems, IEEE-ISCAS*, Atlanta, **2** 81
[5] Jutten C and Hérault J 1988 *Proc. of European Symposium on Signal Processing, EUSIPCO*, Grenoble, France, **2** 643
[6] Jutten C and Hérault J 1991 *Signal Processing* **24** 1
[7] Cichocki A and Unbehauen R 1996 *IEEE Trans. Circuit and Systems-I* **CAS-43** 894
[8] Comon P 1994 *Signal Processing* **36** 287
[9] Comon P and Moreau E 1997 *Proc. Int. Conf. on Acoustics, Speech and Signal Processing, ICASSP*, Münich, Germany, pp. 3453–3456
[10] Moreau E and Macchi O 1996 *Int. J. Adaptive Control and Signal Processing* **10** 19
[11] Cardoso J-F and Laheld B 1996 *IEEE Trans. Signal Processing* **44** (12) 3017
[12] Delfosse N and Loubaton P 1995 *Signal Processing* **45** 59
[13] Thawonmas R, Cichocki A and Amari S I 1998 *IEICE Trans. Fundamentals* **E81-A** (9) 1833
[14] Fiori S 1999 *Network: Computation in Neural Systems* **10** (2) 171
[15] Fiori S 2000 *Neural Networks* **13** (6) 597
[16] Fiori S 2002 *Neural Networks* **15** (1) 71
[17] Pearlmutter B A and Parra L C 1996 *Proc. of Neural Information Processing System, NIPS* (Mozer M M, Jordan M I and Petsche T, Eds), Denver, Colorado, pp. 613–619
[18] Xu L, Cheung C C and Amari S I 1998 *Neurocomputing* (Special issue on Independence and Artificial Neural Networks) **22** (1–3) 69
[19] Cardoso J-F 1999 *Neural Computation* **11** (1) 157

[20] Yeredor A 2000 *Proc. Int. Conf. on Acoustics, Speech and Signal Processing, ICASSP*, Istanbul, pp. 3136–3139
[21] Linsker R 1992 *Neural Computation* **4** 691
[22] Plumbley M D 1993 *Neural Networks* **6** 823
[23] Baram Y and Roth Z 1994 *Technical Report*, CIS-94-20, Center for Intelligent Systems, Technion, Israel Institute for Technology, Haifa
[24] Bell A J and Sejnowski T J 1996 *Neural Computation* **7** (6) 1129
[25] Girolami M and Fyfe C 1997 *IEE Proc. – Vision, Image and Signal Processing* **14** (5) 299
[26] Karhunen J, Oja E, Wang L, Vigário R and Joutsensalo J 1997 *Trans. on Neural Networks* **8** (3) 486
[27] Hyvärinen A and Oja E 1998 *Signal Processing* **64** (3) 301
[28] Fiori S 2000 *Neurocomputing* **34** (1-4) 239
[29] Fiori S 2002 *IEEE Trans. on Neural Networks* **13** (3) 521
[30] Fiori S 2001 *Neural Computation* **13** (7) 1625
[31] Prieto A and Puntonet B 1998 *Signal Processing* **64** (3) 315
[32] Yoshioka M and Omatu S 1998 *Proc. Int. Joint Conf. on Neural Networks, IJCNN*, Anchorage, Alaska, pp. 909–912
[33] Welling M and Weber M 2001 *Neural Computation* **13** (3) 677
[34] Burrascano P, Fiori S and Mongiardo M 1999 *Int. J. RF and Microwave CAE* **9** (3) 158
[35] Sikora R, Chady T and Sikora J 1997 *Int. J. Appl. Electromag. and Mech.* **9** 391
[36] Udpa L and Lord W 1986 *Review of Progress in Quantitative NDE* **5A** 375
[37] Cichocki A and Cao J 1998 *Topics on Non-destructive Evaluation Series* (Djordjevic B B and Reis H D, Eds), The American Society for Non-destructive Evaluation Testing, Inc. **3** 207
[38] Deville Y 1999 *Proc. of Independent Component Analysis Conf., ICA*, Aussois, France, pp. 19–24
[39] Fiori S, Burrascano P, Cardelli E and Faba A 2001 *Proc. 7th Int. Conf. on Engineering Applications of Neural Networks, EANN*, Cagliari, Italy, pp. 188–191
[40] Simone G and Morabito F C 2000 *Proc. Int. Joint Conf. on Neural Networks, IJCNN*, Como, Italy, pp. 59–64
[41] Blitz J 1997 *Electrical and Magnetic Methods of Non-Destructive Testing*, 2nd Ed., Chapman and Hall
[42] Bowler J M 1997 *Int. J. Appl. Electromag. and Mech.* **8** 3
[43] Ypma A 1999 *J. Acoustical Society of the Netherlands* **145** 1
[44] Hyvärinen A and Oja E 2000 *Neural Networks* **13** (4–5) 411
[45] Prince J M and Hildebrand B P 1993 *Applied Optics* **32** (26) 4960